Percolation and jamming of linear k-mers on a square lattice with defects: Effect of anisotropy

Yuri Yu. Tarasevich,[*] Andrei S. Burmistrov,[†] and Taisiya S. Shinyaeva[‡]
Astrakhan State University, 20a Tatishchev Street, Astrakhan 414056, Russia

Valeri V. Laptev[§]
Astrakhan State University, 20a Tatishchev Street, Astrakhan 414056, Russia and Astrakhan State Technical University, 16 Tatishchev Street, Astrakhan 414025, Russia

Nikolai V. Vygornitskii[‖] and Nikolai I. Lebovka[¶]
F. D. Ovcharenko Institute of Biocolloidal Chemistry, NAS of Ukraine, 42 Boulevard Vernadskogo, 03142 Kiev, Ukraine
(Received 2 September 2015; published 28 December 2015)

Using the Monte Carlo simulation, we study the percolation and jamming of oriented linear k-mers on a square lattice that contains defects. The point defects with a concentration d are placed randomly and uniformly on the substrate before deposition of the k-mers. The general case of unequal probabilities for orientation of depositing of k-mers along different directions of the lattice is analyzed. Two different relaxation models of deposition that preserve the predetermined order parameter s are used. In the relaxation random sequential adsorption (RRSA) model, the deposition of k-mers is distributed over different sites on the substrate. In the single-cluster relaxation (RSC) model, the single cluster grows by the random accumulation of k-mers on the boundary of the cluster (Eden-like model). For both models, a suppression of growth of the infinite (percolation) cluster at some critical concentration of defects d_c is observed. In the zero-defect lattices, the jamming concentration p_j (RRSA model) and the density of single clusters p_s (RSC model) decrease with increasing length k-mers and with a decrease in the order parameter. For the RRSA model, the value of d_c decreases for short k-mers ($k < 16$) as the value of s increases. For $k = 16$ and 32, the value of d_c is almost independent of s. Moreover, for short k-mers, the percolation threshold is almost insensitive to the defect concentration for all values of s. For the RSC model, the growth of clusters with ellipselike shapes is observed for nonzero values of s. The density of the clusters p_s at the critical concentration of defects d_c depends in a complex manner on the values of s and k. An interesting finding for disordered systems ($s = 0$) is that the value of p_s tends towards zero in the limits of the very long k-mers, $k \to \infty$, and very small critical concentrations $d_c \to 0$. In this case, the introduction of defects results in a suppression of k-mer stacking and in the formation of empty or loose clusters with very low density. On the other hand, denser clusters are formed for ordered systems with $p_s \approx 0.065$ at $s = 0.5$ and $p_s \approx 0.38$ at $s = 1.0$.

DOI: 10.1103/PhysRevE.92.062142 PACS number(s): 64.60.ah, 68.43.−h, 05.10.Ln, 64.60.De

I. INTRODUCTION

Deposition of large particles such as colloids, polymers, or nanotubes on substrates can be considered and studied as random sequential adsorption (RSA) [1]. During RSA, objects randomly deposit on the substrate; this process is irreversible and the newly adsorbing objects cannot overlap or pass through previously deposited ones. The substrate may be prepatterned (see, e.g., [2]) or include some impurities (defects) (see, e.g., [3]). The adsorbed objects may be identical or present a mixture of objects of different sizes and shapes (see, e.g., [4,5]). Moreover, anisotropy can be introduced by postulating unequal probabilities for the deposition of elongated objects along different axes (see, e.g., [5,6]). The anisotropy of deposition can reflect the influence of external fields, flows, or anisotropy of the substrate. The adsorption of the elongated particles in the presence of external fields produces anisotropic layers (see, e.g., [7,8]).

Very often, during RSA, a substrate can be considered as a discrete space, e.g., a regular or irregular lattice, or as a tree. The simplest but most commonly used instance of a discrete substrate is the square lattice. The objects selected to be adsorbed onto a square lattice are generally linear in shape. Such linear segments (also depicted as needles, linear chains, stiff rods, or k-mers) consist of k successive connected sites.

If deposition of the objects can continue indefinitely, a jamming state is reached. At the jamming state, there are still voids on the substrate between the previously deposited objects, but their sizes or shapes are not sufficient to allow the deposition of even one additional object.

For a perfect lattice (a lattice without any defects), the jamming coverage p_j is the fraction of the sites occupied by deposited objects. For a diluted (disordered and disturbed) lattice (a lattice containing defects or impurities), there are several ways to define the jamming coverage [9–11]. In the present work we use only the pure object jamming limit and defined it as the jamming concentration p_j for short. The pure object jamming limit p_j is defined as the fraction of the total number of lattice sites occupied by the deposited objects [10].

Ben-Naim and Krapivsky obtained an important analytical result for the jamming concentration in a one-dimensional case [9]. If the concentration of the deposited objects on the substrate is sufficiently large, there may be a path through

[*]Corresponding author: tarasevich@asu.edu.ru
[†]ksairen10@mail.ru
[‡]tae4ka19@mail.ru
[§]laptev@ilabsltd.com
[‖]vygor@ukr.net
[¶]Corresponding author: lebovka@gmail.com

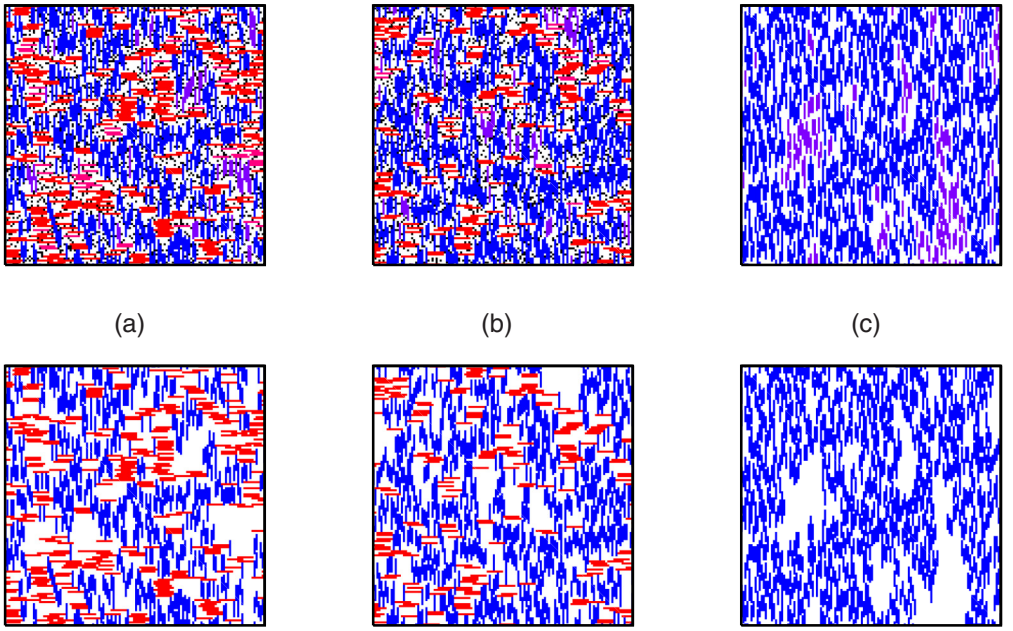

FIG. 1. (Color online) Examples of the jamming states (top row) and the percolation clusters (bottom row) of anisotropically deposited k-mers on a square lattice with defects for (a) $s = 0.25$, (b) $s = 0.5$, and (c) $s = 1$. Both pictures (top and bottom) in each pair (a)–(c) comes from the same Monte Carlo run. The lattice size is 1024×1024, $k = 8$, and a fragment of the lattices with 128×128 sites is shown. The concentration of defects on the lattice is 0.09. The horizontal k-mers are shown in red, vertical k-mers are shown in blue, k-mers not belonging to the percolation cluster are shown in the same colors but with a different hue, empty sites are shown in white, and defects on the lattice are shown in black.

the objects from one side of the system to its opposite side. Below this concentration, there is no spanning path through the system, while above this concentration, there is a connected component of the order of the size of the system. This concentration is called the percolation threshold. (See, e.g., [12] for details; the state of the art may be found, e.g., in [13].) For some systems, percolation never occurs, even at the jamming concentration (e.g., when the adsorbed layer is produced by the deposition of equally sized squares on a square lattice and when the side of the square is greater than the length of three sites [14]). In fact, the percolation threshold corresponds to a phase transition, e.g., an insulator-conductor transition. Different definitions of the percolation threshold are used for lattices with defects similar to the definitions of the jamming concentration. In the present work we use the term percolation threshold p_c as the ratio of the sites occupied by the objects to the total number of lattice sites.

Cornette *et al.* [11,15] investigated numerically the percolation of polyatomic species in the presence of impurities on a square lattice with periodic boundary conditions. Bond and site percolation problems have been taken in consideration. Linear k-mers as well as so-called self-avoiding-walk k-mers, i.e., segments of a self-avoiding walk, have been studied up to $k = 9$. A phase diagram where the critical concentration of impurities is plotted as a function of k has been offered.

The kinetics of the random sequential adsorption of line k-mers (with values of k up to 64) has been studied on a disordered substrate occupied by the point impurities [10]. The coverage of the surface and the jamming limits are calculated by the Monte Carlo method. The coverage has an asymptotically exponential behavior at low concentration of the impurities. The jamming limits depend on the concentrations of the impurities d. At $d < d^*$ the jamming limits decrease as the value of d increases. At $d > d^*$ the jamming limits increase as the value of d increases, where the value of d^* depends on k. In the one-dimensional case, the results are in good agreement with the published analytical results [9]. The coverage and the jamming limits on a two-dimensional disordered lattice are similar to the one-dimensional case. The jamming limits decrease monotonically as the length of the line segments increases.

Recently, the impact of defects on percolation in the random sequential adsorption of linear k-mers on square lattices was investigated for a particularly wide range of k-mers (k-mer lengths from 2 to 256) [16]. Two different cases were studied: (i) where it was assumed that the initial square lattice was nonideal and some fraction d of the sites was occupied by nonconducting point defects (impurities) and (ii) where it was assumed that some fraction d of the sites in the k-mers themselves consisted of defects, i.e., was nonconducting, while the initial square lattice was perfect.

Mixed site-bond percolation was studied for the RSA of k-mers on heterogeneous lattices with variable connectivity z [17]. The simulations were performed for $k = 1$–3 on a triangular lattice. Percolation phase diagrams in terms of the percolation threshold p_c versus lattice connectivity z were obtained. For the RSA deposition of monomers onto a triangular lattice with defects preliminarily filled with k-mers, the percolation ($k = 3$–24) [18] and the jamming ($k \leqslant 50$) [19] were investigated by means of Monte Carlo simulations. The nonmonotonicity of the percolation threshold as a function of the impurity concentration was observed [18].

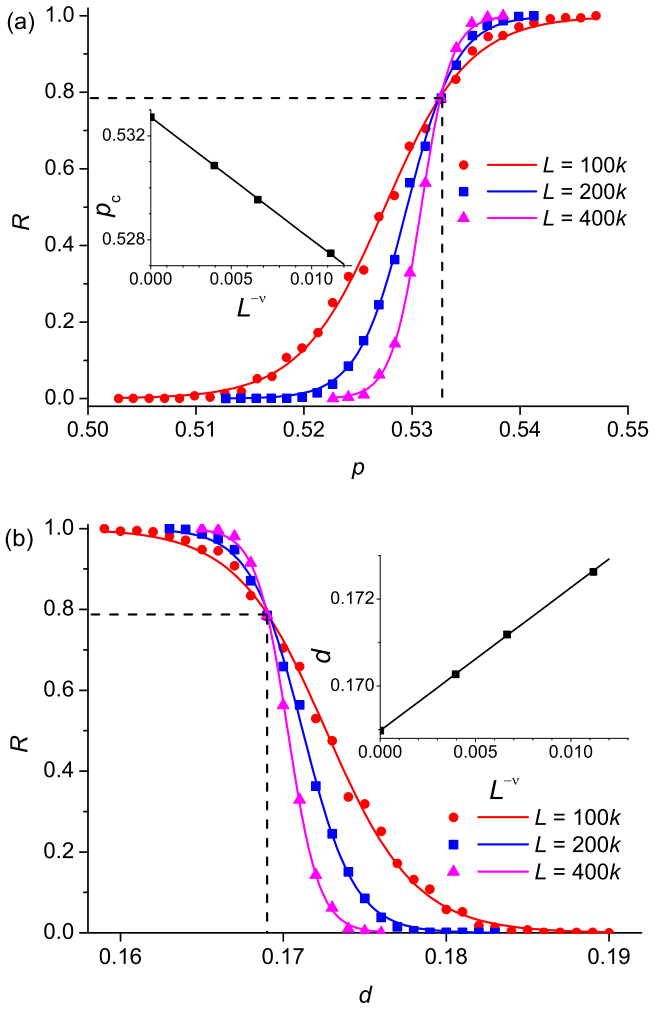

FIG. 2. (Color online) Probability curves for $k = 4$, $s = 0.75$, and the criterion AND: (a) $R(p)$ and (b) $R(d)$. The insets show the scaling. The statistical error is smaller than the marker size.

The RSA of polydisperse mixtures of k-mers has also been extensively investigated [5,20,21]. A phase diagram separating percolating from nonpercolating regions for mixtures of monomers and k-mers on a square lattice ($k = 2$–7) has been also determined [20]. The jamming coverage for a mixture has been found to be greater than the jamming coverage of either of the components making the mixture [5]. On the other hand, the percolation threshold for a mixture was slightly greater than that of the longest k-mer [21]. The continuum random sequential adsorption of a polymer on a flat and homogeneous surface has also been studied [22]. The polymers were modeled as stiff or flexible chains of monomers.

However, most of the previous studies have been devoted to the two-dimensional (2D) deposition of randomly oriented anisometric particles on the substrates. In several works, problems with unequal probabilities for the orientation of the deposition of k-mers along different directions of the lattice have also been analyzed. The degree of anisotropy can be characterized by the order parameter s defined as

$$s = \frac{|N_| - N_-|}{N_| + N_-}, \tag{1}$$

where $N_|$ and N_- are the numbers of vertically and horizontally oriented adsorbed particles.

The anisotropic RSA of dimers on a square lattice has been investigated using Monte Carlo simulation [6,23] and time-series expansion [6]. Data from the Monte Carlo simulations evidence that the orientational order parameter s influences both the values of the percolation threshold p_c and the jamming concentration p_j. In particular, the value of p_j decreases as the order parameter s increases [6,23]. An interesting finding is that in the limit of $s \to 1$, the asymptotic fraction of dimers with horizontal direction does not vanish but equals $e^{-2}[1 - \exp(-2e^{-2})]/2 \approx 0.016\,046$ [6]. The properties of the anisotropic RSA of flexible k-mers on a 2D triangular lattice have been studied numerically by means of Monte Carlo simulations [5]. It was shown that the relaxation time to the jamming limit increases with the degree of anisotropy of the elongated particles.

The effect of anisotropic deposition of k-mers on the jamming [24] and the percolation [25] has also been intensively studied by means of Monte Carlo simulations. These detailed studies revealed that the RSA model does not allow preservation of the order parameter s and in fact the substrate selects the k-mer with appropriate orientation, resulting in deviation of the predetermined order parameter s from the one actually observed one s_0. A special variant of relaxation for the RSA model (the RRSA model) with better preservation of the predetermined anisotropy has been developed [24]. In the RRSA model, the binding of a k-mer to the adsorbing substrate is strong and the k-mer has additional possibilities for joining the surface after an unsuccessful attempt.

The problem of 2D continuous random percolation of conducting sticks (unoriented or partially oriented) has also been the topic of intense study [26–36]. In particular, excluded-volume theory for estimation of the percolation threshold of fully penetrable particles has been widely applied. This theory predicts the following relation for the percolation filling fraction particles φ_c [28,33]:

$$\varphi_c = 1 - \exp(-B_c V / V_{\text{ex}}),$$

where B_c is the number of bounds on one particle, V is the self-volume of the particle, and V_{ex} is the excluded volume of the particle. The value of B_c is commonly estimated from computer simulations.

For rectangular particles $V_{\text{ex}}/V = (4 + \frac{r^2 \sin\gamma}{\pi/4+r})$, where γ is the angle between the particles and $r = L/d$ is an aspect ratio (L is the length and d is the diameter of the particle). For unoriented particles (random orientations) $V_{\text{ex}}/V = 4 + \frac{2r^2/\pi}{\pi/4+r}$ and at $r \gg 1$, $V_{\text{ex}}/V \approx 2r/\pi$. For 2D sticks $B_c = 3.57$–3.7 [28] and one can obtain the following estimation:

$$\varphi_c \approx B_c \pi / 2r.$$

Note that for impenetrable particles with a hard core the probability of direct contact between particles is low and the percolation for this system is absent at any r [37]. However, the percolation is possible for the anisotropic sticks with a core-shell structure [33,38]. The percolation of sticks in 2D continuum deposition models with different rules in spatial correlations between deposited sticks was also studied [36,39].

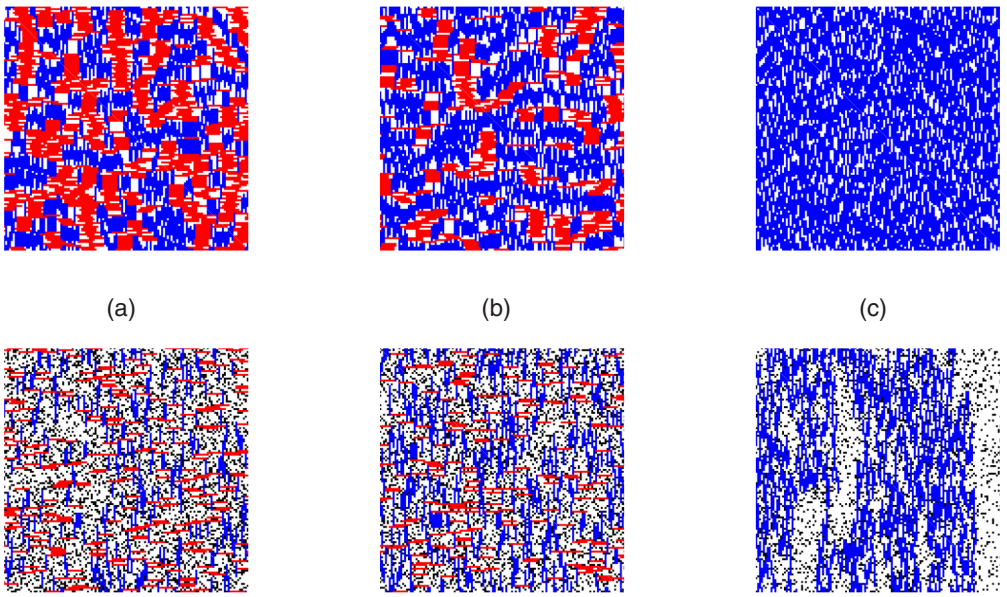

FIG. 3. (Color online) Examples of the clusters in the absence (top row) and in the presence (bottom row) of defects for the RSC model at different values of the order parameter: (a) $s = 0.0$, (b) $s = 0.5$, and (c) $s = 1$. The lattice size is 1024×1024, $k = 8$, and a fragment of the lattices with 128×128 sites is shown. The concentration of defects on the lattice d is near the critical d_c: 0.215 ($s = 0.0$), 0.186 ($s = 0.5$), and 0.134 ($s = 1.0$). The horizontal k-mers are shown in red, vertical k-mers are shown in blue, empty sites are shown in white, and defects on the lattice are shown in black.

Note that in practical applications of colloidal suspensions and deposits on their base the effects of particle clustering (or flocculation) are very important [40]. These interactions were accounted for in different variants of lattice site interactive models [41–46]. In these models the tendency of particles to form clusters is taken into account. The single-cluster model and the flocculation model for continuous fiber deposition were also studied (see [36] for a review).

The present work analyzes the relaxation single-cluster (RSC) and RRSA models. The RSC model is an extension of the Eden growth model [47] for the case of k-mers on a lattice with defects. In the RSC model the cluster grows at its perimeter, starting from an active seed in the center of the lattice, whereas in the RRSA model the deposition is distributed over different sites of the lattice. Our aim is to study the influence of anisotropy on the percolation threshold and the jamming concentration of linear k-mers on a square lattice with point defects. The results for the multiple-cluster RRSA model and the RSC model are compared.

The rest of the paper is organized as follows. Section II describes our RRSA and RSC models of k-mer deposition. The results obtained using finite-size scaling theory and the dependences of the percolation threshold p_c and the jamming concentration p_j vs the order parameter s and the defect concentration d are examined and discussed in detail in Sec. III. We summarize the results in Sec. IV.

II. METHOD

In both the RRSA and the RSC models, the square lattices are initially randomly filled with point defects at a given concentration d. Before deposition of the k-mers, we choose an appropriate orientation in the horizontal or vertical direction according to the given value of the order parameter s. The lattice sites are then occupied by the addition of k-mers. The defects and previously deposited k-mers can inhibit the deposition of newcomers. If the attempt is unsuccessful, a new lattice site (the RRSA model) or a new empty cluster perimeter site (the RSC model) is randomly selected until the object could be deposited. The objects may move over all the substrate (RRSA model) or over all the cluster perimeters (RSC model) searching for a sufficiently large empty space. Additional specific details are presented below.

A. The RRSA model

In the RRSA model, the deposition terminates when a jamming state is reached along one direction [24]. We considered a lattice with periodic (toroidal) boundary conditions to eliminate the border effects and, in contrast to [48], treated spiral clusters as wrapping (percolating). We checked the percolation in two perpendicular directions and used two criteria: There is percolation in both directions (criterion AND) and there is percolation at least along one direction (OR).

Figure 1 presents examples of the jamming states (top row) and the percolation clusters (bottom row) at different values of the order parameter s. The concentration of defects d on the lattice is 0.09.

For each given order parameter s and concentration of defects d we filled the lattice with k-mers to a concentration p or to jamming and checked whether there was percolation. We repeated this 1000 times and found the probability $R(p)$ that percolation occurs at a particular concentration of the k-mers. The abscissa of the inflection point of the curve was treated as the estimate of the percolation threshold for the given lattice size. We used lattices of sizes $L = 100k, 200k, 400k$ and performed finite-size analysis to obtain the percolation threshold at the thermodynamic limit ($L \to \infty$) $p_c \propto L^{-1/\nu}$,

where $\nu = 4/3$ is the critical exponent of the correlation length for the 2D random percolation problem [12]. All probability curves intersect each other at one point with the coordinates (p_c, R^*), where $R^* = R(p_c) \approx 0.78$. The value of R^* depends on how the percolation is defined [48]. The intersection point offers another way to estimate the percolation threshold. The examples of probability curves and scaling are shown in Fig. 2. We compared our numerical simulation for completely aligned k-mers ($s = 1$) with the analytical results [9] and found that there is no visible difference between the analytical and numerical results.

B. The RSC model

The RSC model assumes the presence of strong interactions (attractions) between deposited particles. This model is an extension of the Eden growth model. The Eden algorithm [47] was applied to grow a single cluster from an active seed k-mer on the square lattice. In the RSC model the initial seed k-mer is placed at the center of the lattice and it has $2k + 2$ initial perimeter sites. The RSC algorithm uses the following steps.

Step 1. Randomly choose one empty cluster perimeter site and try to add a new k-mer to any available lattice sites, if such deposition is not inhibited. Repeat this step using the same orientation of the k-mer until the attempt is successful.

Step 2. Determine the new cluster perimeter sites.

Step 3. Repeat the previous steps until there remain no untested cluster perimeter sites or the cluster reaches one of the four boundaries of the lattice.

Examples of clusters in the absence and presence of defects for the RSC model ($k = 8$) with different order parameters s are shown in Fig. 3. When defects are absent, an infinite cluster can grow on the lattice and the formation of stacks of identically oriented k-mers (horizontal and vertical) can be observed. These stacks are rather similar to those observed for the RSA or the RRSA models [24,25]. Visual observations of the patterns at different concentrations of defects allow us to draw the conclusion that the presence of defects restricts the formation of stacks and can prohibit the growth of an infinite single cluster for some critical concentration of defects d_c.

For each given anisotropy s and concentration of defects d we repeated the Monte Carlo experiments 1000 times and found the probability $R_b(d)$ that the single cluster reaches one of the boundaries of the lattice at a given concentration of defects d. We used lattices of different sizes in the interval $L = 8k$–$2048k$. Examples of the probability $R_b(d)$ curves for a disordered system ($s = 0$) using two different values of k are shown in Fig. 4. The values of R_b decrease as the concentration of defects d increases. The commonly applied procedure for determination of the critical concentration d_c for blocking of the cluster growth is to use finite scaling analysis for a fixed value of R_b (e.g., at $R_b = 0.5$). However, for the RSC model the probability $R_b(d)$ curve is not steplike even for infinite systems in the thermodynamic limit $L \to \infty$. For the RSC model at $L \to \infty$, the probability $R_b(d)$ curve smoothly descends as the value of d increases, reflecting the finite probability of the blocking of cluster growth from the initial seed k-mers surrounded by lattice defects. Examples of finite-size analysis at different values of R_b ($k = 2, s = 0$) are presented in Fig. 5(a). Good linear dependences of data were

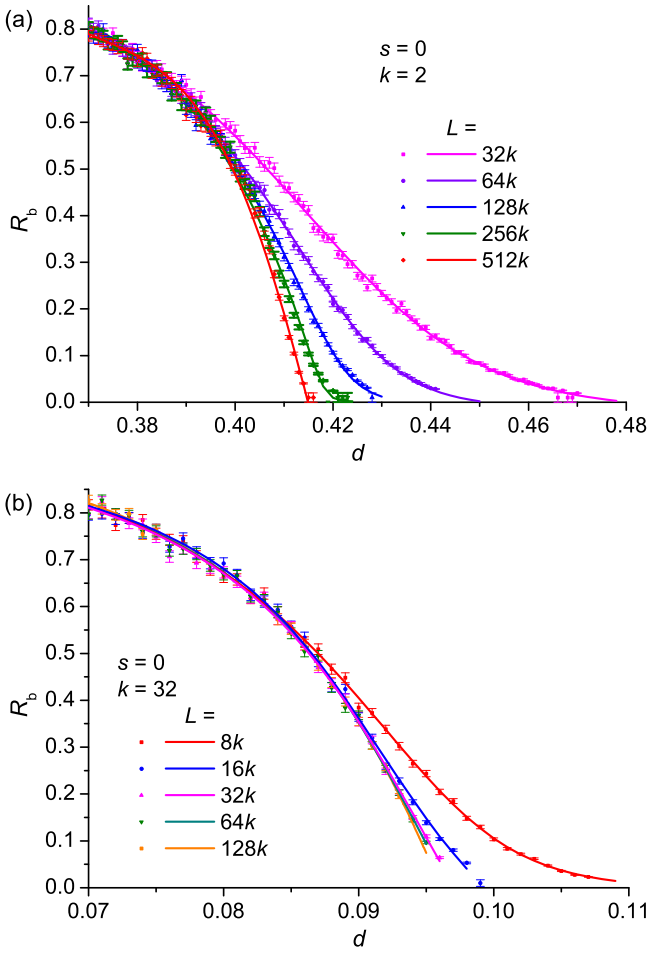

FIG. 4. (Color online) Probability curves $R_b(d)$ for the RSC model with (a) $k = 2$ and (b) $k = 32$. The data are presented for disordered systems $s = 0$. The statistical errors are smaller than the marker size. The lines are provided simply as a guide for the eye.

always observed in the d versus $L^{-1/\nu}$ coordinates, where $\nu = 4/3$ is the critical exponent of the correlation length for the 2D random percolation problem [12]. To be definitive, we always estimate the critical value of the concentration of defects d_c in the limit $L \to \infty$ at the fixed value $R_b = 0.5$ [see Fig. 5(a)]. At this value of d_c, the growth of the infinite cluster is suppressed with a probability of 50%. Examples of the $d(L^{1/\nu})$ dependences for the RSC model ($k = 2$) at different values of the order parameter s ($R_b = 0.5$) are presented in Fig. 5(b). The data show that the slope of the scaling can be greatly dependent on the value of s.

The mean degree of the cluster anisotropy δ has been calculated as

$$\delta = (r_y - r_x)/r, \tag{2}$$

where r_y and r_x are the radii of gyration of the cluster in the y and x directions, respectively, and r is the mean radius of gyration. The density of the cluster of k-mers p_s was calculated inside a rectangle of size $2r_y$ and $2r_x$ with its center located at the geometrical center of the cluster. A finite scaling analysis was also carried out for the estimation of p_s in the limit $L \to \infty$.

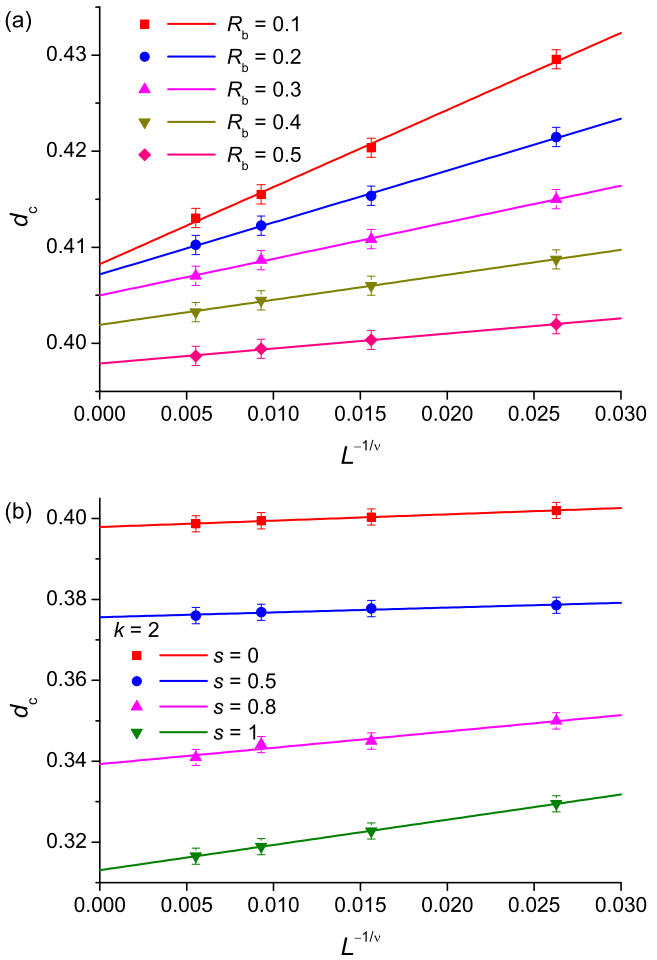

FIG. 5. (Color online) Concentration of defects d_c versus the scaled size of the system $L^{1/\nu}$ for the RSC model ($k = 2$) (a) at different values of probability R_b ($s = 0$) and (b) at different values of the order parameter s ($R_b = 0.5$). Here $\nu = 4/3$ is the critical exponent of the correlation length [12].

III. RESULTS

A. The RRSA model

Figure 6 shows the typical dependences of jamming concentration p_j versus the defect concentration d for different values of k and a fixed value of the order parameter $s = 0.5$. For any given k, the value of p_j decreases as the value of d increases. The effect is more pronounced for the longer k-mers and the jamming concentration decreases drastically with the growth of the k-mer length for any anisotropy. Similar dependences were obtained for other values of the order parameter s.

Figure 7 shows the typical dependences of the relative jamming concentration $p_j/p_j(s = 0)$ versus the order parameter s for different defect concentrations d for $k = 8$. For large concentrations of defects ($d \geqslant 0.25$), the jamming concentration decreases monotonically as the extent of anisotropy increases, whereas for small concentrations of defects ($d < 0.25$), the jamming concentration has a minimum. The minimum depends on d and its position runs from approximately 0.4 ($d \to 0$) to 1.0 ($d \to d^*$), where d^* is between 0.2 and 0.25.

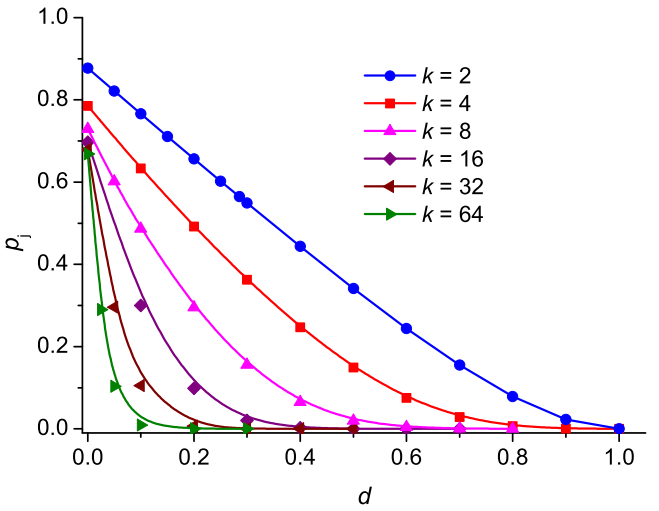

FIG. 6. (Color online) Jamming concentration p_j versus the defect concentration d for different values of k and a fixed order parameter $s = 0.5$. The solid lines are guides for the eye. The statistical error is smaller than the marker size.

In the RRSA model, there exists a critical concentration of defects d_c above which the percolation, i.e., formation of an infinite cluster, is impossible even in the jammed state. An example of the dependences of the percolation threshold p_c and jamming concentration p_j as functions of the defect concentration d for the given order parameter $s = 0.5$ and $k = 2$ is presented in Fig. 8.

For the short k-mers ($k \lessapprox 8$), the percolation threshold p_c is almost insensitive to the defect concentration d for any anisotropy s [49] (see, e.g., Fig. 8 for $k = 2$). The inset in Fig. 8 demonstrates that variation of the percolation threshold does not exceed a few thousandths. For long k-mers ($k > 8$), $p_c(d)$ has a maximum between $d = 0$ and $d = d_c$ [16].

Figure 9 presents percolation phase diagram using as coordinates the critical percolation concentration p_c versus the

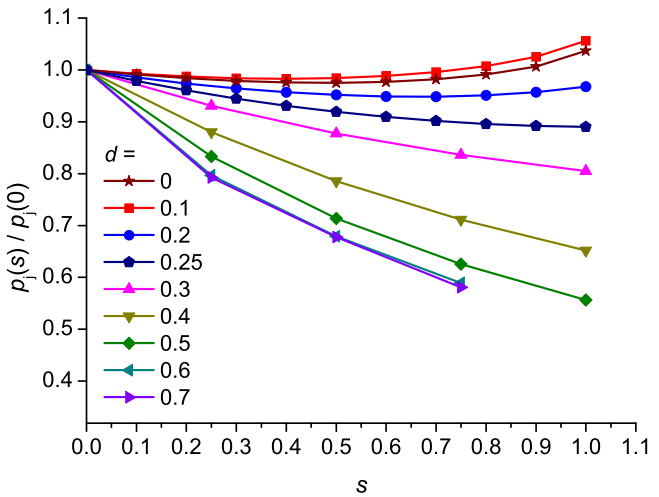

FIG. 7. (Color online) Relative jamming concentration $p_j/p_j(s = 0)$ versus the order parameter s at different concentrations of defects d. The length of the k-mers equals 8. The solid lines are guides for the eye. The statistical error is smaller than the marker size.

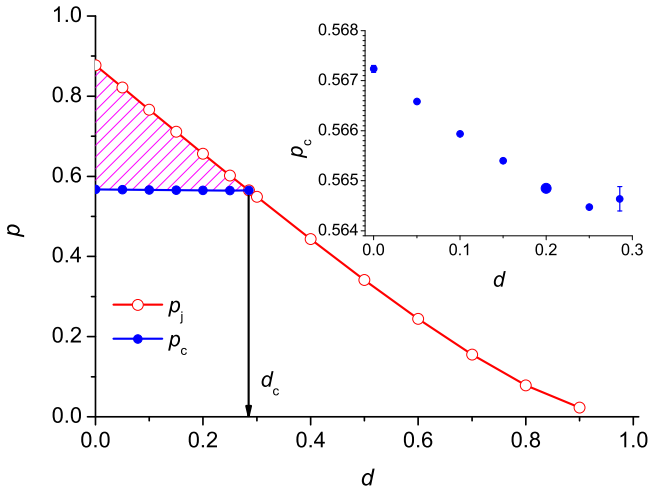

FIG. 8. (Color online) Percolation threshold p_c and jamming concentration p_j as a function of the defect concentration d for the anisotropy $s = 0.5$ and $k = 2$. The hatched region corresponds to the concentrations of the objects and the defects when percolation is possible. Here d_c is a critical concentration of defects that suppresses the formation of an infinite (percolation) cluster. The solid lines are simply guides for the eye. The statistical error is smaller than the marker size when not shown explicitly. The inset shows the percolation threshold p_c as a function of the defect concentration d. The scale of the vertical axis is strongly increased to demonstrate changes in the value of the percolation threshold in the range of a few thousandths.

critical concentration of defects d_c at different values of the order parameter s and lengths of the k-mers. The increase of the order parameter s is always accompanied by an increase of p_c. However, the d_c versus s behavior is different for short and long k-mers. Moreover, it is interesting that for partially oriented systems ($s < 1$) the $p_c(d_c)$ dependences at fixed values of s go through a minimum at the values of k lying in the interval

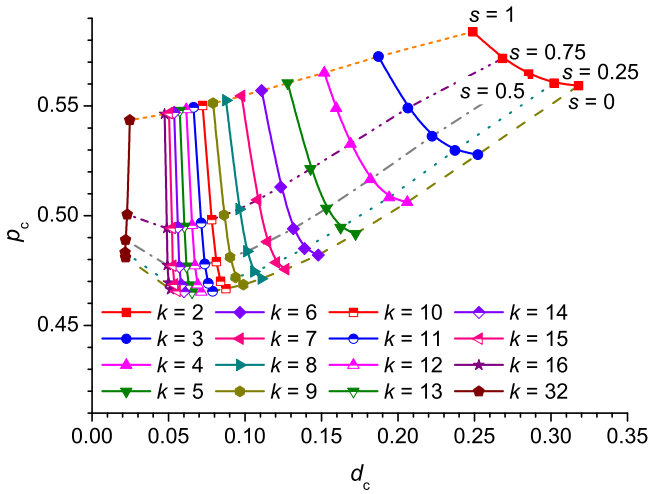

FIG. 9. (Color online) Percolation concentration p_c versus the critical concentration of defects d_c for different values of the order parameter s and lengths of the k-mers. The lines are simply guides for the eye. The statistical error is smaller than the marker size.

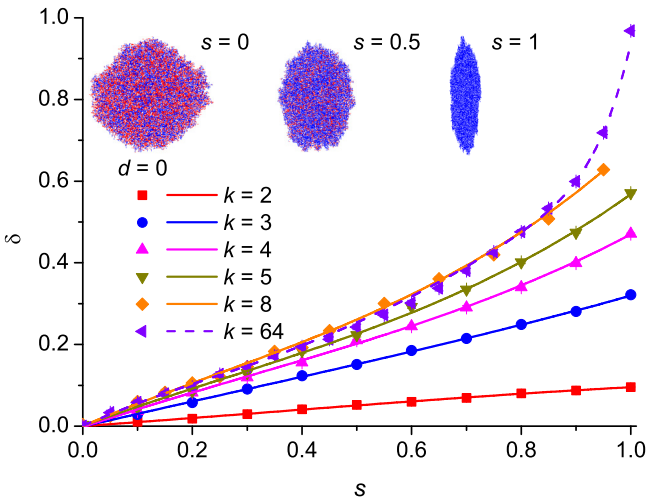

FIG. 10. (Color online) Examples of the degree of the cluster anisotropy δ versus the order parameter s for different values of k for zero-defect lattices ($d = 0$). The inset shows examples of the clusters for $k = 8$.

between 9 and 16. The value of k corresponding the minimum value of d_c increases as the anisotropy increases.

B. The RSC model

Preliminary investigations were performed for zero-defect systems ($d = 0$). Figure 10 presents examples of the degree of the cluster anisotropy δ versus the order parameter s for different values of k for such zero-defect systems ($d = 0$). The value of δ increases as s increases and the effects become more pronounced for the longer k-mers. At large values of s, the shape of the clusters becomes ellipselike (see the inset in Fig. 10).

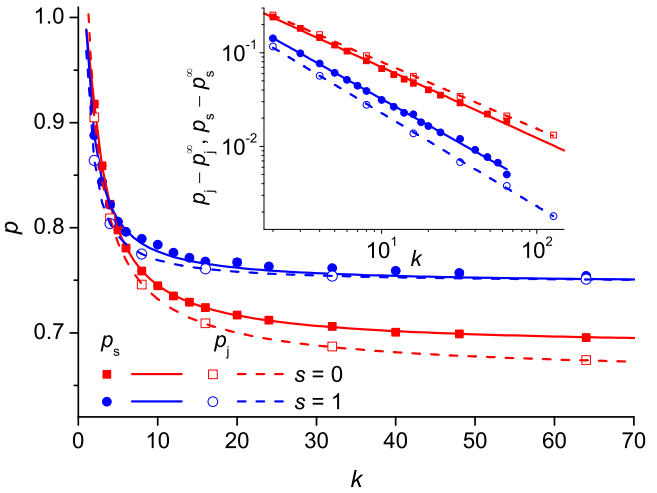

FIG. 11. (Color online) Density of cluster p_s versus the value of k for the RSC model and the jamming concentration p_j versus the value of k for the RRSA model [24]. The data are presented for disordered $s = 0$ and completely ordered $s = 1$ zero-defect systems ($d = 0$). The inset shows $p_s - p_s^\infty$ and $p_j - p_j^\infty$ versus k. Here p_s^∞ and p_j^∞ are the limiting values at $k \to \infty$.

TABLE I. Estimated parameters p_s^∞, p_j^∞, A, and α in the power-law function (3). The data are presented for the RSC and the RRSA [24] models at $s = 0$ and $s = 1$ and for the one-dimensional (1D) model [24]. In all cases the coefficient of determination ρ was greater than 0.999.

	$p_j(k=\infty)$		A		α	
s	RSC	RRSA	RSC	RRSA	RSC	RRSA
0	0.67(6)	0.652(8)	0.41(8)	0.417(5)	0.77(7)	0.713(7)
1	0.745(0)	0.747(2)	0.27(3)	0.235(3)	0.93(1)	1.016(6)
1D	0.74759792		0.227(7)		1.011(1)	

Figure 11 compares both the density of the cluster p_s versus k for the RSC model and the jamming concentration p_j [24] versus k for the RRSA model. It is worth noting that the values of p_s and p_j decrease as an inverse power of the linear segment length k (see the inset in Fig. 11) and approach their limiting values p_s^∞ and p_j^∞ with increasing k:

$$p_{s,j}(k) = p_{s,j}^\infty + A/k^\alpha. \tag{3}$$

The parameters p_s^∞, p_j^∞, A, and α are presented in Table I. The exponent α is not universal and depends upon the order parameter s. It had been suggested that such a power behavior indicates the presence of a fractal structure of the cluster networks in both the RSC and RRSA models with the fractal dimension $d_f = 2 - \alpha$ [24]. For completely ordered systems ($s = 1$), the value of d_f is close to 1 as expected for the 1D problem. For disordered systems at $s = 0$, the values of α are noticeably smaller than 1 for both the RSC and the RRSA models and so the fractal dimension d_f in this case is higher than 1.

Figure 12 compares the density of the cluster p_s versus the concentration of defects d for the RSC model at different values of the linear segment length k for disordered $s = 0$ (solid lines) and completely ordered $s = 1$ (dashed lines) systems. The values of p_s decrease as the value of d increases and there exists some limiting concentration of defects d_c that suppresses the growth of an infinite cluster. At any given value of d, the impact of ordering on the value of p_s depends upon the values of both k and d (Fig. 12).

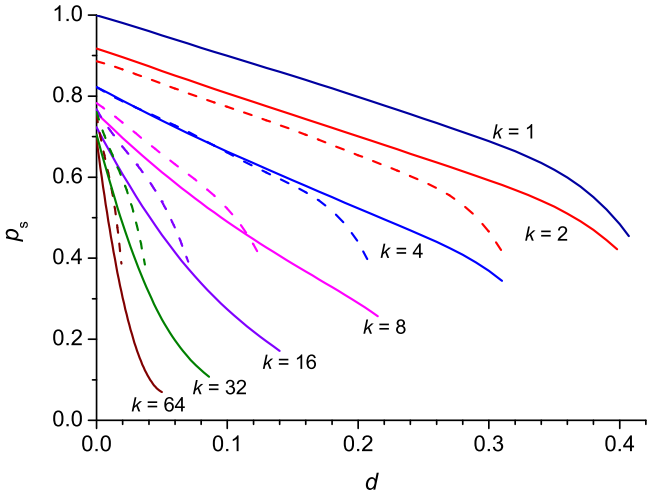

FIG. 12. (Color online) Density of cluster p_s versus the concentration of defects d for the RSC model at different values of the linear segment length k for disordered $s = 0$ (solid lines) and completely ordered $s = 1$ (dashed lines) systems.

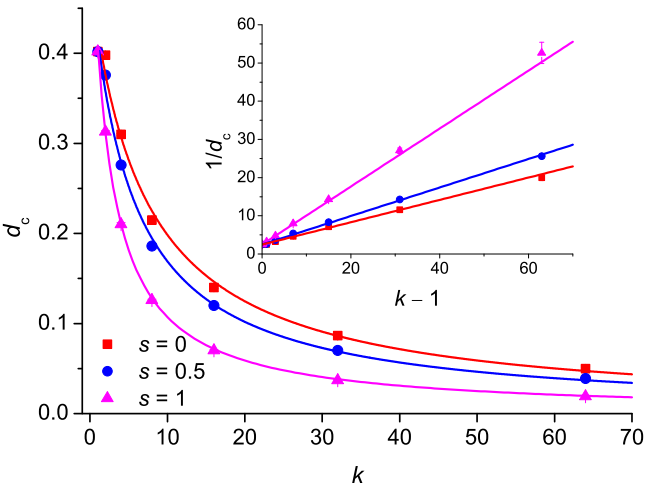

FIG. 13. (Color online) Critical concentration of defects d_c versus the value of k for the RSC model at different values of the order parameter s. The inset shows $1/d_c$ versus $k - 1$ dependences.

The critical concentration of defects d_c decreases as the values of k and s increase and approaches zero in the limit of very long k-mers $k \to \infty$ (Fig. 13). It is interesting that a rather good linear relation between $1/d_c$ and k was observed at different values of s:

$$d_c^{-1} = d_c^{-1}(k=1) + a(k-1), \tag{4}$$

where $d_c^{-1}(k=1) = 2.488 \pm 0.002$, $a = 0.282 \pm 0.004$ ($s = 0.0$), $a = 0.371 \pm 0.004$ ($s = 0.5$), and $a = 0.794 \pm 0.001$ ($s = 1.0$). Note that the value $1 - d_c(k=1) = 0.598 \pm 0.003$ is close to the value of the threshold concentration $\simeq 0.5927$ for ordinary monomer percolation [12].

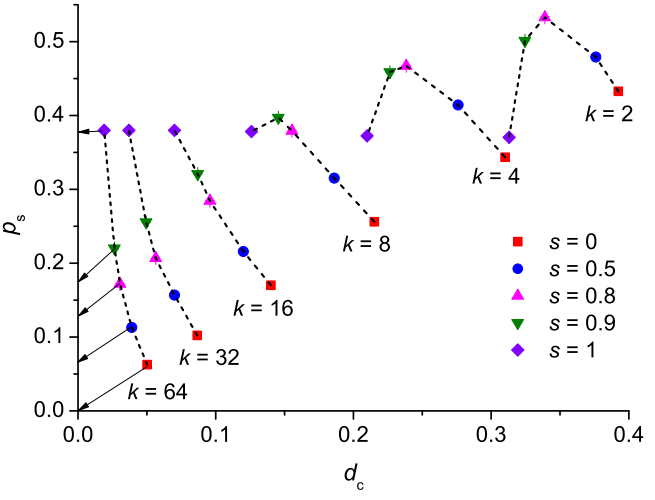

FIG. 14. (Color online) Density of clusters p_s versus the critical concentration of defects d_c for the RSC model at different values of the order parameter s and of k. Arrows show the values of p_s in the limit of very long k-mers $k \to \infty$.

The density of the clusters p_s at the critical concentration of defects d_c for the RSC model depends in a complex manner on s and k (Fig. 14). For disordered systems ($s = 0$), the value of p_s tends to zero in the limits of the very long k-mers $k \to \infty$ and very small critical concentrations $d_c \to 0$. The formation of such empty or loose clusters can be explained by analyzing the cluster patterns presented in Fig. 3. In zero-defect systems ($d = 0$), compact clusters form with significant stacks of identically oriented k-mers (horizontal and vertical). These stacks are responsible for the high values of p_s. The introduction of defects strongly prevents the formation of stacks [see, e.g., Fig. 3(a)] and loose networks with near zero density are formed. On the other hand, denser clusters are formed for ordered systems with $p_s \approx 0.065$ at $s = 0.5$ and $p_s \approx 0.38$ at $s = 1.0$.

IV. CONCLUSION

For the problem of k-mer deposition, the RRSA and RSC models have huge differences in their deposition rules and structure of the clusters they generate. In the RRSA model, random deposition of k-mers is performed, with multiple clusters being formed that can be consolidated in the course of their growth. Intensive studies with the RRSA have shown that the jamming concentration continuously decreases as the lengths of the k-mers increase [24]. The percolation threshold initially decreases and then increases with increasing value of k [25]. For a completely disordered system, i.e., at $s = 0$, a conjecture has been offered that the formation of an infinite cluster is impossible when k exceeds approximately 1.2×10^4 [25]. On the other hand, in the RSC model the single cluster grows at its perimeter by an Eden growth process [47] and the formation of an infinite cluster is not restricted for any values of k. This model assumes strong attractions of the newcomer to the previously deposited particles at their lateral boundaries. The Eden-like clusters display noticeable shape anisotropy at high values of the order parameter s.

It is amazing that, in spite of these differences between the RRSA and RSC models, they display some general similarities. In the absence of defects on the substrate (for zero-defect systems $d = 0$) the jamming concentration p_j for the RRSA model and density of the cluster p_s for the RSC model display similar dependences on the linear segment length k and on the order parameters (see Fig. 12). The impacts of defects on the percolation and jamming characteristics are also fairly similar. For both models the suppression of the growth of an infinite (percolation) cluster at some critical concentration of defects d_c can be observed. Phase diagrams in the form of the $p_c(d_c)$ (RRSA model) and $p_s(d_c)$ dependences for different values of s and k were determined.

For the RRSA model, the value of p_c ranges in the interval $\approx$0.465–0.58 ($k = 2$–32) and the value of d_c decreases for short k-mers ($k < 16$) but increases for long k-mers ($k > 16$) as the value of s increases. For the RRSA model, the value of d_c decreases for short k-mers ($k < 16$) as the value of s increases. For $k \geqslant 16$, the value of d_c is almost independent of s. Moreover, for short k-mers, the percolation threshold is almost insensitive to the defect concentration for any values of s. For the RSC model the value of p_s at the critical concentration of defects d_c depends in a complex manner on the values of s and k. For disordered systems ($s = 0$), the value of p_s tends to zero in the limits of very long k-mers $k \to \infty$. This reflects a suppression of k-mer stacking by the defects that results in the formation of loose clusters with very low density.

ACKNOWLEDGMENTS

The reported study was partially supported by the Russian Foundation for Basic Research, Project No. 14-02-90402_Ukr_a; the Ministry of Education and Science of the Russian Federation, Project No. 643; and the National Academy of Sciences of Ukraine, Project No. 43-02-14(U).

[1] J. W. Evans, Random and cooperative sequential adsorption, Rev. Mod. Phys. **65**, 1281 (1993).
[2] A. Cadilhe, N. A. M. Araújo, and V. Privman, Random sequential adsorption: From continuum to lattice and pre-patterned substrates, J. Phys.: Condens. Matter **19**, 065124 (2007).
[3] J. W. Lee, Effects of impurities in random sequential adsorption on a one-dimensional substrate, Phys. Rev. E **55**, 3731 (1997).
[4] J. W. Lee, Irreversible random sequential adsorption of mixtures, Colloids Surf. A **165**, 363 (2000).
[5] L. Budinski-Petković, I. Lončarević, Z. M. Jakšić, S. B. Vrhovac, and N. M. Švrakić, Simulation study of anisotropic random sequential adsorption of extended objects on a triangular lattice, Phys. Rev. E **84**, 051601 (2011).
[6] M. J. de Oliveira, T. Tomé, and R. Dickman, Anisotropic random sequential adsorption of dimers on a square lattice, Phys. Rev. A **46**, 6294 (1992).
[7] I. Pagonabarraga, J. Bafaluy, and J. M. Rubí, Adsorption of Colloidal Particles in the Presence of external Fields, Phys. Rev. Lett. **75**, 461 (1995).
[8] I. Pagonabarraga, J. Bafaluy, and J. M. Rubí, Adsorption kinetics in the presence of external fields, Phys. Rev. E **59**, 4285 (1999).
[9] E. Ben-Naim and P. L. Krapivsky, On irreversible deposition on disordered substrates, J. Phys. A **27**, 3575 (1994).
[10] J. W. Lee, Kinetics of random sequential adsorption on disordered substrates, J. Phys. A **29**, 33 (1996).
[11] V. Cornette, A. J. Ramirez-Pastor, and F. Nieto, Percolation of polyatomic species with the presence of impurities, J. Chem. Phys. **125**, 204702 (2006).
[12] D. Stauffer and A. Aharony, *Introduction to Percolation Theory* (Taylor & Francis, London, 1992).
[13] N. Araújo, P. Grassberger, B. Kahng, K. J. Schrenk, and R. M. Ziff, Recent advances and open challenges in percolation, Eur. Phys. J. ST **223**, 2307 (2014).
[14] M. Nakamura, Percolational and fractal property of random sequential packing patterns in square cellular structures, Phys. Rev. A **36**, 2384 (1987).
[15] V. Cornette, A. J. Ramirez-Pastor, and F. Nieto, Random sequential adsorption of polyatomic species with the presence of impurities, Physica A **390**, 671 (2011).

[16] Y. Y. Tarasevich, V. V. Laptev, N. V. Vygornitskii, and N. I. Lebovka, Impact of defects on percolation in random sequential adsorption of linear k-mers on square lattices, Phys. Rev. E **91**, 012109 (2015).
[17] M. Quintana, I. Kornhauser, R. López, A. J. Ramirez-Pastor, and G. Zgrablich, Monte Carlo simulation of the percolation process caused by the random sequential adsorption of k-mers on heterogeneous triangular lattices, Physica A **361**, 195 (2006).
[18] G. Kondrat, The study of percolation with the presence of impurities, J. Chem. Phys. **122**, 184718 (2005).
[19] G. Kondrat, The effect of impurities on jamming in random sequential adsorption of elongated objects, J. Chem. Phys. **124**, 054713 (2006).
[20] M. Dolz, F. Nieto, and A. J. Ramirez-Pastor, Percolation processes in monomer-polyatomic mixtures, Physica A **374**, 239 (2007).
[21] L. Budinski-Petković, I. Lončarević, M. Petković, Z. M. Jakšić, and S. B. Vrhovac, Percolation in random sequential adsorption of extended objects on a triangular lattice, Phys. Rev. E **85**, 061117 (2012).
[22] M. Cieśla, Continuum random sequential adsorption of polymer on a flat and homogeneous surface, Phys. Rev. E **87**, 052401 (2013).
[23] V. A. Cherkasova, Y. Y. Tarasevich, N. I. Lebovka, and N. V. Vygornitskii, Percolation of aligned dimers on a square lattice, Eur. Phys. J. B **74**, 205 (2010).
[24] N. I. Lebovka, N. N. Karmazina, Y. Y. Tarasevich, and V. V. Laptev, Random sequential adsorption of partially oriented linear k-mers on a square lattice, Phys. Rev. E **84**, 061603 (2011).
[25] Y. Y. Tarasevich, N. I. Lebovka, and V. V. Laptev, Percolation of linear k-mers on a square lattice: From isotropic through partially ordered to completely aligned states, Phys. Rev. E **86**, 061116 (2012).
[26] G. E. Pike and C. H. Seager, Percolation and conductivity: A computer study. I, Phys. Rev. B **10**, 1421 (1974).
[27] I. Balberg and N. Binenbaum, Computer study of the percolation threshold in a two-dimensional anisotropic system of conducting sticks, Phys. Rev. B **28**, 3799 (1983).
[28] I. Balberg, C. H. Anderson, S. Alexander, and N. Wagner, Excluded volume and its relation to the onset of percolation, Phys. Rev. B **30**, 3933 (1984).
[29] P. C. Robinson, Connectivity of fracture systems—A percolation theory approach, J. Phys. A: Math. Gen. **16**, 605 (1983).
[30] P. C. Robinson, Numerical calculations of critical densities for lines and planes, J. Phys. A: Math. Gen. **17**, 2823 (1984).
[31] A. L. R. Bug, S. A. Safran, and I. Webman, Continuum Percolation of Rods, Phys. Rev. Lett. **54**, 1412 (1985).
[32] A. L. R. Bug, S. A. Safran, and I. Webman, Continuum percolation of permeable objects, Phys. Rev. B **33**, 4716 (1986).
[33] I. Balberg and N. Binenbaum, Invariant properties of the percolation thresholds in the soft-core–hard-core transition, Phys. Rev. A **35**, 5174 (1987).
[34] W. J. Boudville and T. C. McGill, Finite-size effects in two-dimensional continuum percolation, Phys. Rev. B **39**, 369 (1989).
[35] C. Vanneste, A. Gilabert, and D. Sornette, Finite-size effects in line-percolating systems, Phys. Lett. A **155**, 174 (1991).
[36] N. Provatas, M. Haataja, J. Asikainen, S. Majaniemi, M. Alava, and T. Ala-Nissila, Fiber deposition models in two and three spatial dimensions, Colloid Surf. A **165**, 209 (2000).
[37] S. P. Obukhov, Percolation in a system of randomly distributed sticks, J. Phys. A: Math. Gen. **21**, 3975 (1988).
[38] L. Berhan and A. M. Sastry, Modeling percolation in high-aspect-ratio fiber systems. I. Soft-core versus hard-core models, Phys. Rev. E **75**, 041120 (2007).
[39] J. Asikainen and T. Ala-Nissila, Percolation and spatial correlations in a two-dimensional continuum deposition model, Phys. Rev. E **61**, 5002 (2000).
[40] B. Dobias and H. Stechemesser, *Coagulation and Flocculation*, 2nd ed. (CRC, Boca Raton, 2005).
[41] L. J. Duckers and R. G. Ross, Percolation with non-random site occupation, Phys. Lett. A **49**, 361 (1974).
[42] L. J. Duckers, Percolation with nearest neighbor interaction, Phys. Lett. A **67**, 93 (1978).
[43] J. W. Evans, J. A. Bartz, and D. E. Sanders, Multicluster growth via irreversible cooperative filling on lattices, Phys. Rev. A **34**, 1434 (1986).
[44] D. E. Sanders and J. W. Evans, Correlated percolation in island-forming processes: Analysis of cooperative filling on a square lattice, Phys. Rev. A **38**, 4186 (1988).
[45] S. R. Anderson and F. Family, Percolation in an interactive cluster-growth model, Phys. Rev. A **38**, 4198 (1988).
[46] J. W. Evans, From lattice to continuum percolation via clustering, J. Phys. A: Math. Gen. **23**, L197 (1990).
[47] M. Eden, *Proceedings of Fourth Berkeley Symposium on Mathematics, Statistics, and Probability* (University of California Press, Berkeley, 1961), Vol. 4, pp. 223–239.
[48] M. E. J. Newman and R. M. Ziff, Fast Monte Carlo algorithm for site or bond percolation, Phys. Rev. E **64**, 016706 (2001).
[49] Y. Y. Tarasevich, V. V. Laptev, A. S. Burmistrov, and T. S. Shinyaeva, Influence of anisotropy on percolation and jamming of linear k-mers on square lattice with defects, J. Phys. Conf. Ser. **633**, 012064 (2015).